BIOCHEMISTRY
including biophysical chemistry & molecular biology

ARTICLE

pubs.acs.org/biochemistry

# Interaction and Inhibitory Effect of Ammonium Cation in the Oxygen Evolving Center of Photosytem II

Masaya Tsuno,[‡] Hiroyuki Suzuki,[‡,§] Toru Kondo,[†] Hiroyuki Mino,[†] and Takumi Noguchi*[,†,‡]

[†]Division of Material Science, Graduate School of Science, Nagoya University, Furo-cho, Chikusa-ku, Nagoya 464-8602, Japan

[‡]Institute of Materials Science, University of Tsukuba, Tsukuba, Ibaraki 305-8573, Japan

[§]Department of Biology, Faculty of Science, Tokyo University of Science, Kagurazaka 1-3, Shinjuku-ku, Tokyo 162-8601, Japan

**ABSTRACT:** Photosynthetic $O_2$ evolution takes place at the Mn cluster in photosystem II (PSII) by oxidation of water. It has been proposed that ammonia, one of water analogues, functions as an inhibitor of $O_2$ evolution at alkaline pH. However, the detailed mechanism of inhibition has not been understood yet. In this study, we investigated the mechanism of ammonia inhibition by examining the $NH_4Cl$-induced inhibition of $O_2$ evolution in a wide pH range (pH 5.0−8.0) and by detecting the interaction site using Fourier transform infrared (FTIR) spectroscopy. In addition to intact PSII membranes from spinach, PSII membranes depleted of the PsbP and PsbQ extrinsic proteins were used as samples to avoid the effect of the release of these proteins by salt treatments. In both types of samples, oxygen evolution activity decreased by approximately 40% by addition of 100 mM $NH_4Cl$ in the range of pH 5.0−8.0. The presence of inhibition at acidic pH without significant pH dependence strongly suggests that $NH_4^+$ cation functions as a major inhibitor in the acidic pH region, where neutral $NH_3$ scarcely exists in the buffer. The $NH_4Cl$ treatment at pH 6.5 and 5.5 induced prominent changes in the $COO^-$ stretching regions in FTIR difference spectra upon the $S_1 \rightarrow S_2$ transition measured at 283 K. The $NH_4Cl$ concentration dependence of the amplitude of the spectral changes showed a good correlation with that of the inhibition of $O_2$ evolution. From this observation, it is proposed that $NH_4^+$ cation interacts with carboxylate groups coupled to the Mn cluster as direct ligands or proton transfer mediators, causing inhibition of the $O_2$ evolving reaction.

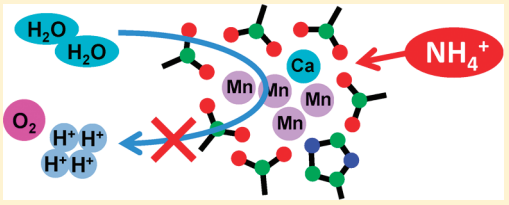


Photosynthetic oxygen evolution by plant and cyanobacteria takes place at the oxygen evolving center (OEC) in photosystem II (PSII) protein complexes.[1−4] The X-ray crystallographic structures of the PSII core complexes from thermophilic cyanobacteria at 2.9−3.5 Å resolution[5−7,a] together with the information from EXAFS studies[8] revealed that the OEC consists of a $Mn_4Ca$ cluster surrounded by carboxylate and histidine ligands. In the OEC, two water molecules are converted into one molecular oxygen and four protons through a light-driven cycle, the so-called S-state cycle, consisting of five intermediates ($S_i$ states; $i = 0−4$).[1−4] Among them, the $S_1$ state is the most stable in the dark, and flash illumination advances each $S_i$ ($i = 0−3$) state to the next $S_{i+1}$ state. The $S_4$ state is a transient intermediate and relaxes to the $S_0$ state, releasing molecular oxygen. The molecular mechanism of water oxidation, however, remains largely unknown.

One promising method for investigation of the oxygen-evolving mechanism is to examine the mechanism of inhibition by water analogues. Ammonia has been known as one of such water analogues, and its effects on the structure and reaction of OEC have been extensively studied. Early studies using chloroplasts by Hind and co-workers,[9,10] in which the pH dependence of the reduction rates of artificial electron acceptors was examined upon addition of $NH_4Cl$, proposed the idea that $NH_3$ as a neutral base, in equilibrium with $NH_4^+$ cation ($pK_a = 9.25$), is the species responsible for the inhibition. After these works, most of the experiments of ammonia inhibition have been performed at alkaline pH. Velthuys[11] showed by delayed luminescence measurements that ammonia is bound in the $S_2$ and $S_3$ states and inhibits the $S_3 \rightarrow S_0$ transition. Thermoluminescence data by Ono and Inoue[12] also showed the binding of ammonia in the $S_2$ state lowering its oxidation potential and the blockage of the $S_3 \rightarrow S_0$ transition. Sandusky and Yocum[13,14] examined the inhibitory effect of ammonia in competition with $Cl^-$ and found that there are two ammonia binding sites; the first site is identical to the $Cl^-$ binding site and is common to other amines, while the second site is specific to ammonia. Using EPR spectroscopy, Brudvig and co-workers[15,16] showed that this second site induced an altered multiline signal, suggesting direct binding of ammonia to the Mn cluster in the $S_2$ state. The altered multiline signal, which was almost saturated with 100 mM $NH_4Cl$,[15] was detected by annealing to 0 °C after illumination at 210 K, providing evidence that ammonia binding to the Mn site occurs in the $S_2$ state. Britt et al.[17] further proposed from the ESEEM study that an amido ($NH_2$) bridge is formed between the Mn ions. This proposal was consistent with the EXAFS data by Dau et al.,[18] which showed elongation of the one binuclear center by 0.15 Å.

Boussac et al.[19] further analyzed the ammonia inhibition using EPR and steady-state $O_2$ evolution and found that inhibition was

**Received:** December 7, 2010
**Revised:** February 20, 2011
**Published:** February 21, 2011

observed neither under strong continuous illumination nor under very low light or flash illumination. They explained this observation as indicating that, at high light intensity, the S states turn over so rapidly that ammonia binding cannot take place, and at very low light intensity, the ammonia bound in the $S_2$ state is rapidly exchanged by water upon $S_4$ formation. It was proposed that an ammonia molecule bound in the $S_2$ state providing the altered multiline signal does not directly cause the inhibition of the S-state turnover but the second ammonia molecule that binds in the $S_3$ state blocks the $S_3 \rightarrow S_0$ transition.[19,20] The absence of direct correlation between the altered multiline EPR signal and the inhibition of $O_2$ evolution was also suggested by Andréasson et al.[21]

Light-induced FTIR difference spectroscopy is another powerful method to investigate the structure and molecular interactions in OEC.[22−26] Using this technique, Chu and co-workers[27,28] showed that $NH_4Cl$ treatment at pH 7.5 induced a clear change in the $S_2/S_1$ difference spectrum obtained at 250 K. A positive band at 1365 $cm^{-1}$, which can be assigned to the symmetric stretching band of a carboxylate group in the $S_2$ state, upshifted by 14 $cm^{-1}$. From the observations that this change was not detected at 200 K and saturated with 100 mM $NH_4Cl$, which is similar to the behaviors of the altered multiline EPR signal, they proposed that the change in the FTIR signal has the same origin as the altered multiline signal and is caused by the binding of ammonia to the Mn cluster.[27,28]

In spite of the above extensive studies on the ammonia inhibition, the exact binding site of ammonia and the detailed mechanism of inhibition have not been clarified yet. In this study, we have investigated the molecular mechanism of ammonia inhibition of $O_2$ evolution by examining the $NH_4Cl$-induced effect on $O_2$ evolution in a wide pH range (pH 5.0−8.0) and detecting the ammonia interaction in OEC at a physiological temperature using light-induced FTIR difference spectroscopy. Except for early studies using chloroplasts,[9,10] the pH dependence of ammonia inhibition has not been reported so far for isolated PSII samples. In addition to intact PSII membranes from spinach, we used PSII membranes depleted of the PsbP and PsbQ proteins to avoid the effect of the release of these extrinsic proteins by $NH_4Cl$ and NaCl (as a control) treatment. The result showed that $NH_4Cl$-induced inhibition was observed not only at alkaline pH but also in the acidic pH region, suggesting that $NH_4^+$ cation, rather than neutral $NH_3$, functions as a major inhibitor in the latter region. Furthermore, FTIR difference spectra in the $S_1 \rightarrow S_2$ transition measured at pH 6.5 and 5.5 at 283 K revealed the interaction of $NH_4^+$ to carboxylate groups coupled to the Mn cluster, which may cause the inhibition of $O_2$ evolution. The interaction site at 283 K was different from that at 250 K, which has been observed by Chu et al.[27,28]

## MATERIALS AND METHODS

**Sample Preparations.** Oxygen evolving PSII membranes of spinach[29] were prepared following the method previously described[30] and suspended in pH 6.5 buffer containing 40 mM Mes, 400 mM sucrose, 20 mM $CaCl_2$ and 15 mM NaCl (buffer A). Depletion of the PsbP and PsbQ extrinsic proteins was performed by NaCl washing,[30,31] in which the sample was incubated in a buffer containing 2 M NaCl (40 mM Mes−NaOH, 400 mM sucrose, 20 mM $CaCl_2$, and 2 M NaCl, pH 6.5) for 20 min on ice, followed by washing twice with buffer A by centrifugation. The presence or absence of extrinsic proteins (PsbP, PsbQ, and PsbO) was examined by SDS−PAGE with 15% acrylamide gel containing 6 M urea. For pH dependence experiments, 40 mM Mes (pH 5.0−7.0) or Hepes (pH 7.5−8.0) buffers with other components identical to buffer A were used for the PsbP, PabQ-depleted PSII samples, while the same buffers but without $CaCl_2$ were used for intact PSII samples. Note that addition of 100 mM or lower concentration of $NH_4Cl$ to each buffer did not shift the pH by more than 0.1. As for buffers containing 500 mM and 1 M $NH_4Cl$, pH was adjusted in the presence of $NH_4Cl$.

**Measurements of Oxygen Evolution Rates.** The $O_2$ evolution rate of the PSII samples was measured using a Clark-type oxygen electrode at 25 °C. The 10 $\mu$L sample (1 mg of Chl/mL) in buffer A was mixed with 980 $\mu$L of measuring buffer (final sample concentration: 10 $\mu$g of Chl/mL), and 10 $\mu$L of 100 mM P*p*BQ/DMSO (final P*p*BQ concentration: 1 mM) was added as an electron acceptor. A couple of measurements were performed at each condition, and the data were averaged.

**FTIR Measurements.** For $S_2/S_1$ FTIR measurements at 283 K, the sample (0.5 mg of Chl/mL) in buffer A at pH 6.5 or corresponding buffer at pH 5.5 with an indicated amount of $NH_4Cl$ or NaCl and 20 mM potassium ferricyanide was centrifuged at 170000*g* for 30 min, and the resulting pellet was sandwiched between two $CaF_2$ plates (25 mm diameter). One of the $CaF_2$ plates has a circular groove (14 mm inner diameter; 1 mm width), and the sample cell was sealed with silicone grease laid on the outer part of the groove.[32] The sample temperature was adjusted to 283 K by circulating cold water in a copper holder. The sample was stabilized at this temperature in the dark for 3 h before recording spectra. Flash-induced $S_2/S_1$ FTIR difference spectra were recorded using a Bruker IFS-66/S spectrophotometer and a Q-switched Nd:YAG laser (Quanta-Ray GCR-130; 532 nm, ∼7 ns fwhm).[32] Two preflashes (1 Hz) were applied to the sample to synchronize all centers to the $S_1$ state, reduce the nonheme iron to $Fe^{2+}$, and oxidize $Y_D$. After 5 min, single-beam spectra (20 s scans) were recorded before and after a single flash (∼7 mJ/$cm^2$ per pulse) followed by dark relaxation for 5 min. This cycle was repeated 80 times, and averaged spectra were used to calculate a flash-induced difference spectrum representing an $S_2/S_1$ difference.

FTIR measurements at 250 K were performed as described in ref 33. For $S_2Q_A^-/S_1Q_A$ measurements, PSII membranes (0.5 mg of Chl/mL) in buffer A with additional 100 mM NaCl or $NH_4Cl$ was supplemented with 0.1 mM DCMU and centrifuged at 170000*g* for 30 min. The resulting pellet was sandwiched between two $CaF_2$ plates (13 mm in diameter). In the case of $Q_A^-/Q_A$ measurement, Mn-depleted PSII membranes prepared by $NH_2OH$ treatment were suspended in buffer A and supplemented with 10 mM $NH_2OH$ (as an exogenous electron donor) and 0.1 mM DCMU before centrifugation. The temperature was adjusted to 250 K in a cryostat (Oxford DN1704) using a controller (Oxford ITC-5). Single-beam spectra (150 s scans) were recorded before and after continuous white light illumination for 10 s from a halogen lamp (Hoya-Schott, HL-150R; ∼40 mW/$cm^2$ at the sample), and difference spectra were calculated. Two spectra were averaged for final data. All FTIR spectra were recorded at 4 $cm^{-1}$ resolution.

**EPR Measurements.** EPR spectra were measured at 4.7 K on a Bruker ESP-300E EPR spectrometer with a gas flow temperature control system (Oxford, CF935). A standard resonator (ER4102) was used. The PspP, PspQ-depleted PSII membranes (∼6 mg of Chl/mL) in buffer A and those in the presence of 100 mM NaCl or $NH_4Cl$ were supplemented with 0.1 mM DCMU. The $S_2$ state was formed by illumination at 250 K by

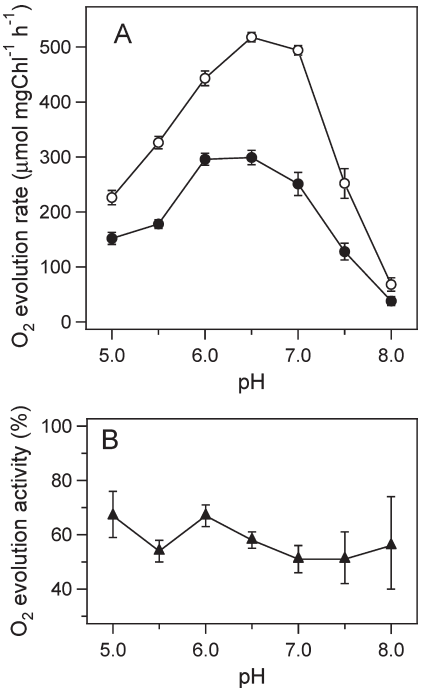


**Figure 1.** (A) The pH dependence of the $O_2$ evolution rates of PSII membranes in the presence of 100 mM $NH_4Cl$ (closed circles) and 100 mM NaCl instead of $NH_4Cl$ (open circles). The buffers contain 40 mM Mes (pH 5.0−7.0) or Hepes (pH 7.5−8.0), 400 mM sucrose, and 15 mM NaCl with additional NaCl or $NH_4Cl$. As an electron acceptor, 1 mM P*p*BQ was also added to the buffer. The temperature was 25 °C. (B) The pH dependence of the relative $O_2$ evolution activity (%) of the PSII membranes in the presence of 100 mM $NH_4Cl$ with respect to that of the control samples with 100 mM NaCl.

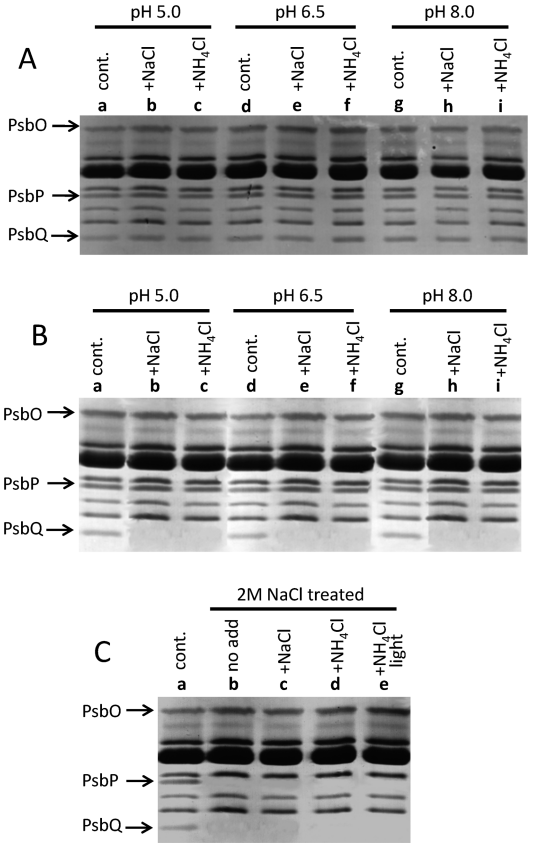


**Figure 2.** SDS−PAGE analysis of the extrinsic proteins in PSII membranes from spinach. (A, B) Untreated (a, d, g) and 100 mM NaCl (b, e, h) and 100 mM $NH_4Cl$ (c, f, i) treated PSII samples at pH 5.0 (a−c), pH 6.5 (d−f), and pH 8.0 (g−i). The samples were treated under dark (A) and incubated under room light for 40 min on ice (B). (C) PsbP, PsbQ-depleted PSII membranes by 2 M NaCl wash (b−e) in comparison with control PSII membranes (a). PsbP, PsbQ-depleted PSII with no addition (b), 1 M NaCl (c), and 1 M $NH_4Cl$ (d, e) at pH 6.5. The sample (e) was incubated under room light for 40 min on ice after $NH_4Cl$ treatment.

continuous illumination from a LED lamp (Hayashi Watch-Works, LA-HDF158A; 480 mW/cm$^2$ at the sample) for 1 min.

## RESULTS

Figure 1A shows the pH dependence of the $O_2$ evolution rate of PSII membranes from spinach in buffers in the presence of 100 mM $NH_4Cl$ (closed circles) and 100 mM NaCl as a control (open circles). In both plots, the $O_2$ evolution rate exhibits a bell-shape pH dependence of $O_2$ evolution with lower rates at acidic and alkaline regions. Such a bell-shape pH dependence has been shown in previous measurements of $O_2$ evolution for PSII preparations.[34] Figure 1B shows the $O_2$ evolution activity of the $NH_4Cl$-treated sample relative to that of the control (NaCl-treated) sample as a function of pH. The relative activities of $NH_4Cl$-treated samples were about 60% in the examined pH range (pH 5.0−8.0). Although the buffers used for this experiment did not contain $CaCl_2$ to minimize the salt effect on the extrinsic proteins, a very similar result was obtained using buffers in the presence of 20 mM $CaCl_2$ (data not shown). Boussac et al.[19] previously reported that ammonia inhibition at pH 7.6 was observed neither at very strong nor very weak (or flash) illumination and required moderate-intensity illumination. With the same moderate light intensity used for both control and $NH_4Cl$-treated samples, the $O_2$ evolution activity was close to the maximum value in the former sample whereas it decreased by ∼40% in the latter sample.[19] In our experiment, such a moderate light condition was verified by the observation that the relative activity of $NH_4Cl$-treated PSII at pH 6.5 was virtually unchanged when the light intensity was halved (from 190 to 95 mW/cm$^2$). It is notable that the relative activity of ∼60% in our result is in good agreement with the value observed by Boussac et al.[19] in 100 mM $NH_4Cl$-treated sample at pH 7.6 using moderate-intensity light.

It has been previously reported that 50 mM $NH_4Cl$ treatment under room light at pH 7.5−7.6 fully or partially removes the PsbQ and PsbP extrinsic proteins.[35] It is hence possible that the above relative $O_2$ evolution activities include the effect of the release of these extrinsic proteins. We have examined the presence of extrinsic proteins in our samples by SDS−PAGE analysis. Although the samples treated with 100 mM NaCl and 100 mM $NH_4Cl$ under dark retained all of the extrinsic proteins (PsbO, P, Q) at any pH (pH 5.0−8.0) (Figure 2A), both samples showed the release of the PsbQ protein after exposure to room light for 40 min on ice (Figure 2B). This observation indicates that the PsbQ protein is readily released during illumination in the $O_2$ evolution measurement. To examine the real $NH_4Cl$ effect without the salt effect of releasing the extrinsic proteins, in the following experiments we used PSII membranes in which the PsbP and PsbQ proteins were removed in advance by 2 M NaCl wash. Using such samples is also necessary to examine the $NH_4Cl$

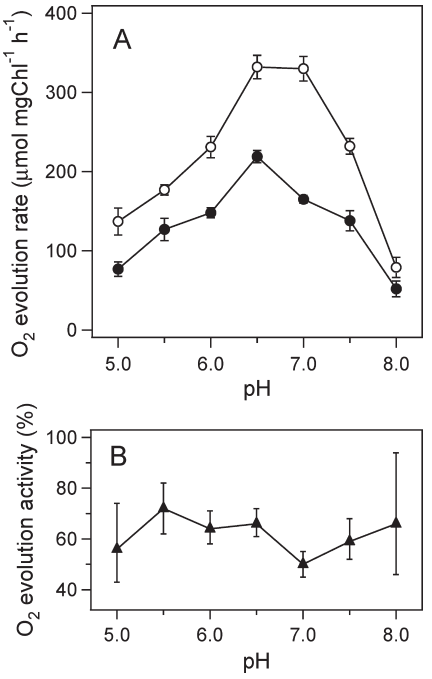


**Figure 3.** (A) The pH dependence of the $O_2$ evolution rates of PsbP, PsbQ-depleted PSII membranes in the presence of 100 mM $NH_4Cl$ (closed circles) and 100 mM NaCl instead of $NH_4Cl$ (open circles). Conditions other than the presence of 20 mM $CaCl_2$ in buffers were the same as for Figure 1A. (B) The pH dependence of the relative $O_2$ evolution activity (%) of the PsbP, PsbQ-depleted PSII membranes in the presence of 100 mM $NH_4Cl$ with respect to that of the control samples with 100 mM NaCl.

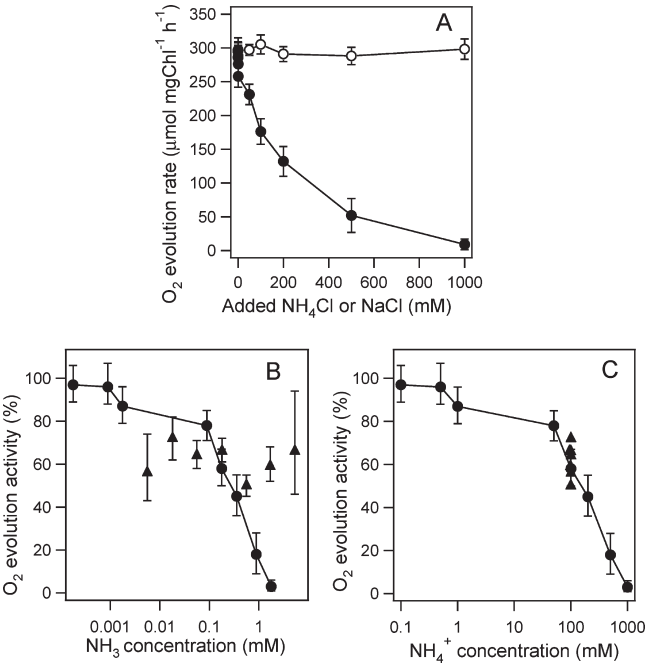


**Figure 4.** (A) Dependence on $NH_4Cl$ concentration of the $O_2$ evolution rate of PsbP, PsbQ-depleted PSII membranes at pH 6.5 (closed circles) in comparison with the $O_2$ evolution rate of the control sample (open circles) containing NaCl instead of $NH_4Cl$. (B, C) Relative $O_2$ evolution activities (%) plotted as a function of $NH_3$ concentration (B) and $NH_4^+$ concentration (C), using the data of different $NH_4Cl$ concentrations at pH 6.5 (closed circles) and those of 100 mM $NH_4Cl$ at pH 5.0−8.0 (closed triangles). Error bars for the data of different pHs in (C) are omitted.

concentration dependence, which requires higher concentration $NH_4Cl$ treatment.

Figure 3A shows the pH dependence of the $O_2$ evolution rate of PsbP, PsbQ-depleted PSII membranes in the presence of 100 mM $NH_4Cl$ (closed circles) and 100 mM NaCl (open circles). Note that the buffers contained sufficient amounts of $Ca^{2+}$ (20 mM) and $Cl^-$ (155 mM) to support the $O_2$ evolution of the PsbP, PsbQ-depleted PSII. The pH dependence of the $O_2$ evolution rate showed a bell shape similar to that of the intact PSII retaining the PsbP and PsbQ proteins. The generally lower $O_2$ evolving rates than those of intact PSII (e.g., 332 $\mu$mol (mg of Chl)$^{-1}$ h$^{-1}$ at pH 6.5 in comparison with 507 $\mu$mol (mg of Chl)$^{-1}$ h$^{-1}$ in intact PSII) are consistent with previous observations.[30,36] Figure 3B shows the $O_2$ evolution activity of the $NH_4Cl$-treated sample relative to that of the control (NaCl-treated) sample as a function of pH. The relative activity was about 60% in the range of pH 5.0−8.0 in fair agreement with that of the intact PSII (Figure 1B). This result indicates that the $O_2$ evolution activity is decreased by about 40% by 100 mM $NH_4Cl$ treatment without significant pH dependence.

In the next experiment, we examined the dependence of the inhibition of $O_2$ evolution on the $NH_4Cl$ amount added to the PsbP, PsbQ-depleted PSII membranes. The concentration of $NH_4Cl$ in buffer was changed from 0.1 mM to 1 M while fixing the pH to 6.5. In the control measurement, the same amount of NaCl, instead of $NH_4Cl$, was added to the sample. This type of experiment can be accomplished only by using PsbP, PsbQ-depleted PSII samples without the salt effect on the extrinsic proteins. No release of the PsbO protein from the PsbP, PsbQ-depleted PSII by 1 M $NH_4Cl$ treatment (and 1 M NaCl treatment as a control) was confirmed by SDS−PAGE analysis (Figure 2C). The obtained result is shown in Figure 4A. As the concentration of $NH_4Cl$ increased, the $O_2$ evolution rate decreased (closed circles), whereas no effect was observed by increasing the NaCl concentration (open circles). These data clearly show the inhibitory effect of $NH_4Cl$ at pH 6.5.

The relative activities as a function of concentration of $NH_3$ (Figure 4B) and $NH_4^+$ (Figure 4C) in equilibrium with each other ($pK_a$ = 9.25) were plotted using the data of the $NH_4Cl$ concentration change at pH 6.5 (closed circles; deduced from Figure 4A) and those of the pH change (pH 5.0−8.0) with 100 mM $NH_4Cl$ (closed triangles; deduced from Figure 3B). It is clear that the plots as a function of the $NH_3$ concentration (Figure 4B) do not agree between the former and the latter data sets, whereas in the plots of the $NH_4^+$ concentration dependence (Figure 4C), both sets of data were consistent with each other.

Figure 5A shows the effect of $NH_4Cl$ on the FTIR difference spectrum upon the $S_1 \rightarrow S_2$ transition ($S_2/S_1$ difference) of the PsbP, PsbQ-depleted PSII membranes. The sample was in a buffer at pH 6.5, and the temperature was 283 K. Spectra of the PSII samples treated with 1000 (a), 500 (b), 100 (c), and 50 (d) mM $NH_4Cl$ (red lines) are compared with those of the control samples that were treated with the same amount of NaCl (black lines). In $S_2/S_1$ difference spectra, prominent bands in the 1700−1600, 1600−1500, and 1450−1300 cm$^{-1}$ regions have been assigned to the amide I (the C═O stretches of backbone amides), amide II (the NH bends coupled with the CN stretches of backbone amides)/asymmetric $COO^-$ stretching, and symmetric $COO^-$ stretching vibrations, respectively.[25,26,37,38] The


dx.doi.org/10.1021/bi101952g |*Biochemistry* 2011, 50, 2506–2514

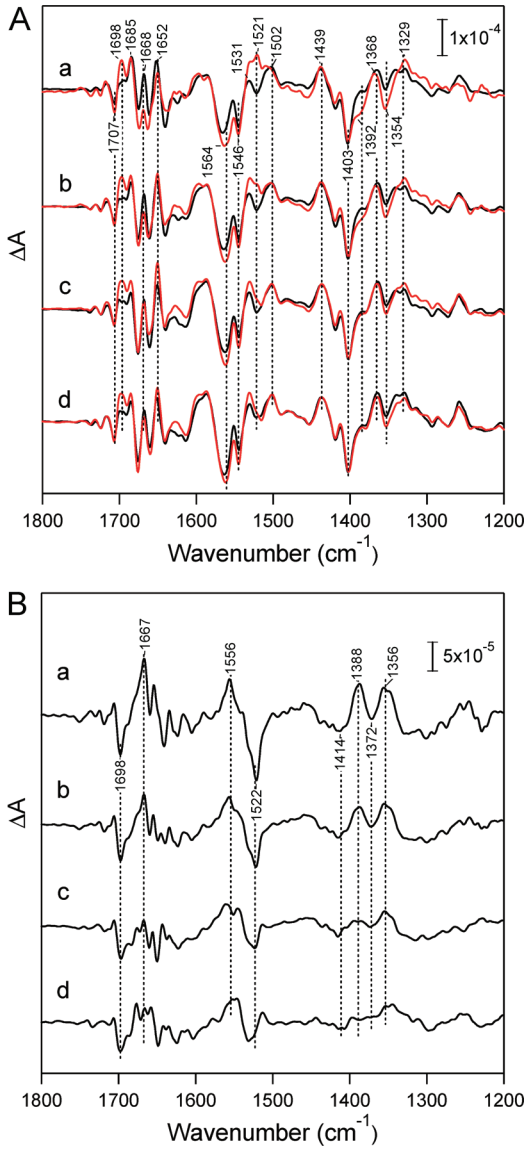


**Figure 5.** (A) Flash-induced $S_2/S_1$ FTIR difference spectra of PsbP, PsbQ-depleted PSII membranes in a pH 6.5 buffer in the presence of $NH_4Cl$ (red lines) compared with the control spectra in the presence of NaCl (black lines). (B) Double difference spectra between the $S_2/S_1$ spectra of $NH_4Cl$- and NaCl-treated PSII membranes at pH 6.5 (NaCl minus $NH_4Cl$). The concentrations of $NH_4Cl$ or NaCl in samples were 1000 (a), 500 (b), 100 (c), and 50 (d) mM. The sample temperature was adjusted to 283 K.

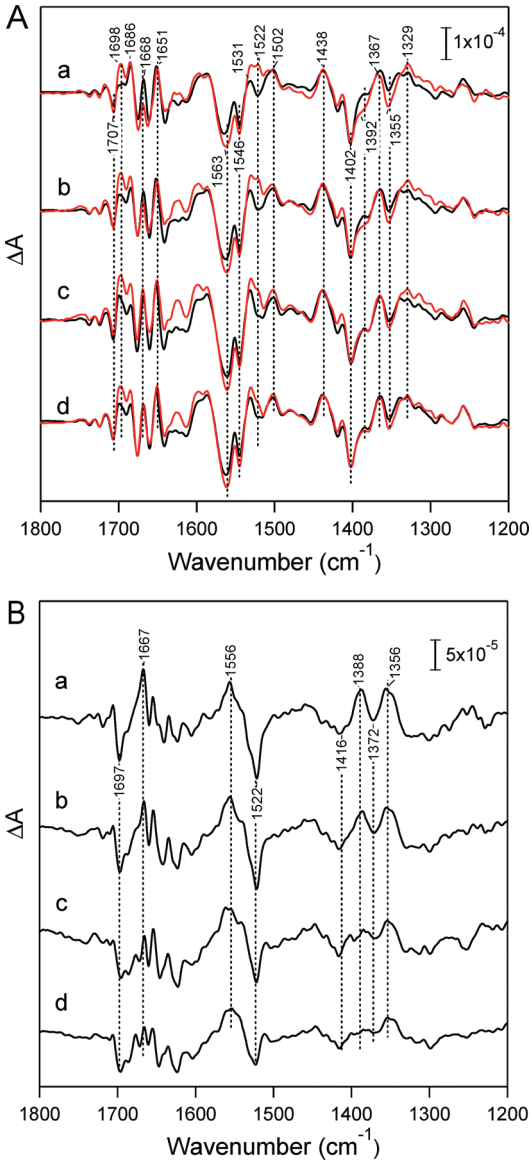


**Figure 6.** (A) Flash-induced $S_2/S_1$ FTIR difference spectra of PsbP, PsbQ-depleted PSII membranes in a pH 5.5 buffer in the presence of $NH_4Cl$ (red lines) compared with the control spectra in the presence of NaCl (black lines). (B) Double difference spectra between the $S_2/S_1$ spectra of $NH_4Cl$- and NaCl-treated PSII membranes at pH 5.5 (NaCl minus $NH_4Cl$). The concentrations of $NH_4Cl$ or NaCl in samples were 1000 (a), 500 (b), 100 (c), and 50 (d) mM. The sample temperature was adjusted to 283 K.

control spectra are virtually identical to the previous $S_2/S_1$ spectrum of PsbP, PsbQ-depleted PSII membranes,[39] which showed characteristic changes in the amide I region when compared with the spectrum of an intact PSII sample. No appreciable changes were detected by increasing the concentration of NaCl from 50 mM to 1 M (Figure 5Aa−d, black lines), although on a closer look, there are small changes in the relative peak intensities in the amide I region (1700−1600 $cm^{-1}$), which is generally sensitive to sample conditions. In contrast, upon addition of 1 M $NH_4Cl$, some clear changes were observed in the whole region (Figure 5Aa). In the symmetric $COO^-$ region, negative features at 1392 and 1354 $cm^{-1}$ and a positive band at 1329 $cm^{-1}$ increased the intensities. Also, in the asymmetric $COO^-$/amide II regions, a positive band appeared at 1521 $cm^{-1}$, and the negative band at ∼1564 $cm^{-1}$ showed a stronger intensity. Furthermore, in the amide I region, a positive peak at 1668 $cm^{-1}$ decreased the intensity, and a positive band appeared at 1698 $cm^{-1}$. These changes diminished as the concentration of $NH_4Cl$ was lowered (Figure 5Ab−d, red lines).

The $NH_4Cl$-induced spectral changes are more clearly expressed in double difference spectra between the spectra of $NH_4Cl$- and NaCl-treated samples (NaCl minus $NH_4Cl$; Figure 5B). In the double difference spectra between 1 M $NH_4Cl$ and NaCl (Figure 5Ba), clear bands were observed at 1414(−)/1388 (+)/1372(−)/1356(+), 1556(+)/1522(−), and 1698(−)/1667-(+) $cm^{-1}$ in the symmetric $COO^-$, asymmetric $COO^-$/amide II,


dx.doi.org/10.1021/bi101952g |*Biochemistry* 2011, 50, 2506–2514

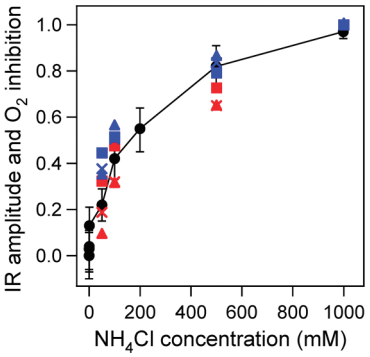


**Figure 7.** The relative amplitudes of the $NH_4Cl$-induced FTIR bands at pH 6.5 (red marks) and pH 5.5 (blue marks) plotted as a function of $NH_4Cl$ concentration, in comparison with the inhibition ratio of $O_2$ evolution (black circle). Key: triangles, the 1522 $cm^{-1}$ band ($\Delta A$ difference from 1500 $cm^{-1}$); crosses, the 1388 $cm^{-1}$ band ($\Delta A$ difference from 1414 $cm^{-1}$); squares, the 1356 $cm^{-1}$ band ($\Delta A$ difference from 1372 $cm^{-1}$). The inhibition ratio was deduced from the $O_2$ evolution activity as a function of the $NH_4Cl$ concentration in Figure 4A.

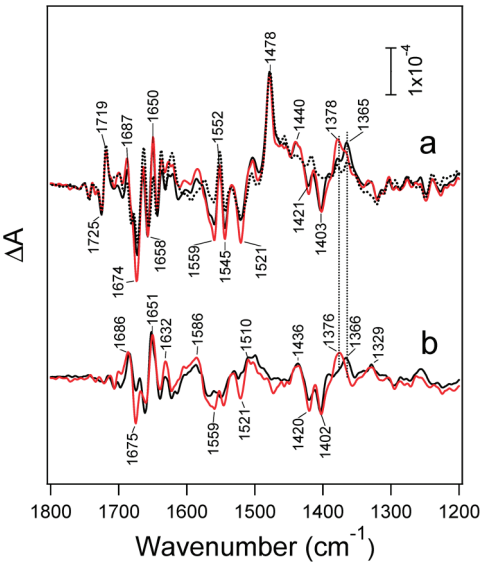


**Figure 8.** (a) $S_2Q_A^-/S_1Q_A$ FTIR difference spectrum of the PsbP, PsbQ-depleted PSII membranes treated with 100 mM $NH_4Cl$ (red solid line) measured at 250 K in a pH 6.5 buffer in comparison with the control spectrum in the presence of 100 mM NaCl (black solid line). The $Q_A^-/Q_A$ difference spectrum of the PsbP, PsbQ-depleted PSII measured at 250 K was superimposed (black dotted line). (b) $S_2/S_1$ difference spectra (black line, +100 mM NaCl; red line, +100 mM $NH_4Cl$) calculated by taking the double difference of $Q_A^-/Q_A$ and $S_2Q_A^-/S_1Q_A$ difference spectra ($S_2Q_A^-/S_1Q_A$ minus $Q_A^-/Q_A$).

and the amide I regions, respectively. The intensities of these bands decreased as the concentration of $NH_4Cl$ deceased (Figure 5Ba–d). It should be noted that the virtually identical $NH_4Cl$-induced changes were observed using PsbP, PsbQ-intact PSII membranes by addition of 100 mM $NH_4Cl$ (data not shown), indicating that the observed spectral changes are not attributed to the absence of extrinsic proteins.

Figure 6 shows the $S_2/S_1$ spectra of NaCl- and $NH_4Cl$-treated samples in a buffer at pH 5.5 and their double difference spectra, respectively. The spectral features were very similar to those at

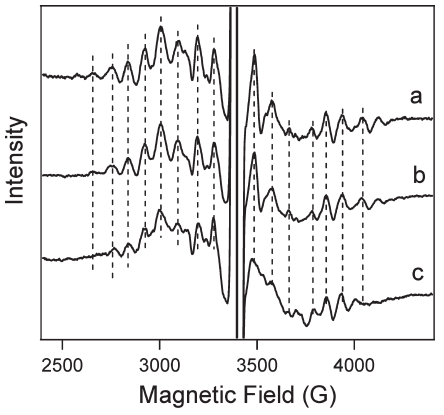


**Figure 9.** Multiline EPR spectra of the $S_2$ state in the PspP, PspQ-depleted PSII membranes (a) and those treated with 100 mM NaCl (b) and 100 mM $NH_4Cl$ (c) in a pH 6.5 buffer. Samples in the presence of 0.1 mM DCMU were illuminated at 250 K to produce the $S_2$ state. Measurement conditions: temperature, 4.7 K; microwave frequency, 9.52 GHz; microwave power, 0.8 mW; modulation amplitude, 20 G.

pH 6.5 (Figure 5), indicating that the $NH_4Cl$ effects on the FTIR spectra are basically independent of pH in this acidic pH region.

Figure 7 shows the plots of the relative amplitudes of the $NH_4Cl$-induced bands at 1522 (triangles), 1388 (crosses), and 1356 (squares) $cm^{-1}$ in the $COO^-$ stretching region of the double difference spectra at pH 6.5 (red marks) and pH 5.5 (blue marks) as a function of $NH_4Cl$ concentration together with the inhibition ratio of $O_2$ evolution (black circles) deduced from Figure 4A (1 − relative $O_2$ activity). It is clearly shown that the FTIR changes are well correlated with the inhibition ratio. It is worth noting that with 1.5 M $NH_4Cl$ concentration the $S_2/S_1$ FTIR signals significantly decreased concomitant with the appearance of the nonheme iron signals[40] as major features, suggesting the destruction of the Mn cluster by the treatment with very high concentration of $NH_4Cl$.

The $S_2/S_1$ difference spectra at 250 K were obtained by measuring $S_2Q_A^-/S_1Q_A$ and $Q_A^-/Q_A$ difference spectra and taking double difference. The reason for using this method to obtain the $S_2/S_1$ difference spectra without using ferricyanide as an electron acceptor is that the signals of the nonheme iron preoxidized by ferricyanide contaminate the spectra at pH 6.5.[40] At 283 K such contamination was avoided by introducing preflashes and repeating the measurements with intervals of 5 min. Figure 8a shows $S_2Q_A^-/S_1Q_A$ FTIR difference spectra of the PsbP, PsbQ-depleted PSII samples measured at 250 K. The samples were in a pH 6.5 buffer in the presence of either 100 mM NaCl (black solid line) or 100 mM $NH_4Cl$ (red solid line). The $Q_A^-/Q_A$ difference spectrum of PsbP, PsbQ-depleted PSII was also presented (black dotted line). The $S_2/S_1$ spectra calculated as $S_2Q_A^-/S_1Q_A$ minus $Q_A^-/Q_A$ double difference spectra are presented in Figure 8b (black line, 100 mM NaCl; red line, 100 mM $NH_4Cl$). The 1366 $cm^{-1}$ band in the symmetric $COO^-$ region exhibited a clear upshift to 1376 $cm^{-1}$ by 100 mM $NH_4Cl$ treatment, in agreement with the previous observation by Chu et al.[27,28] for intact (in the presence of PsbP and PsbQ) PSII samples at pH 7.5. The very similar upshift from 1365 to 1375 $cm^{-1}$ was also observed at pH 5.5 (data not shown). Thus, the FTIR change at 250 K seems to be dependent neither on the PsbP and PsbQ proteins nor on pH. It is notable that this spectral change was not detected in the corresponding $S_2/S_1$ difference spectra measured at 283 K (Figures 5Ac and 6Ac).


dx.doi.org/10.1021/bi101952g |*Biochemistry* 2011, 50, 2506–2514

Figure 9 shows the multiline EPR spectra of the $S_2$ state in the PspP, PspQ-depleted PSII membranes (a) and those treated with 100 mM NaCl (b) and 100 mM $NH_4Cl$ (c) in a pH 6.5 buffer. The $S_2$ state was produced by illumination at 250 K, and the spectra were measured at 4.7 K. It was shown that the multiline signal was not significantly modified by addition of 100 mM $NH_4Cl$ at pH 6.5. Although each line was slightly broadened (Figure 9c), the peak positions were virtually unchanged compared with the control spectra without and with 100 mM NaCl (Figure 9a and 9b, respectively). This is a sharp contrast to the previous spectra of PSII treated with 100 mM $NH_4Cl$ at ~pH 7.5, which showed reduced spacing of hyperfine lines.[15,16,19]

## DISCUSSION

In this study, we examined the $NH_4Cl$-induced inhibition of $O_2$ evolution using PSII membranes from spinach at various pHs. In both intact and PsbP, PsbQ-depleted PSII membranes, treatment of 100 mM $NH_4Cl$ induced a decrease in the $O_2$ evolution activity by approximately 40% in the range of pH 5.0−8.0 (Figures 1B and 3B). In intact PSII membranes, however, salt effects on the extrinsic proteins are inevitable. Kuntzleman and Haddy[35] reported full or partial release of PsbQ and PsbP proteins by 50 mM $NH_4Cl$ treatment under room light in the presence of 0−15 mM $CaCl_2$ at alkaline pH. We also observed the release of PsbQ by both 100 mM NaCl and 100 mM $NH_4Cl$ treatment in the absence of $CaCl_2$ under room light at pH 5.0−8.0 (Figure 2B). Hence, the $NH_4Cl$ effect in intact PSII possibly includes the effect of destabilized extrinsic proteins on $O_2$ evolution activity. By contrast, in the experiments using the PsbP, PsbQ-depleted PSII membranes, there was no concern about the release of these extrinsic proteins by salt treatments. We confirmed that the PsbO protein was not affected even by 1 M $NH_4Cl$ treatment (Figure 2C). Thus, the results obtained using PsbP, PsbQ-depleted PSII (Figures 3 and 4) should provide a pure effect of $NH_4Cl$ on $O_2$ evolution.

With the p$K_a$ value of 9.25 for the equilibrium between $NH_4^+$ and $NH_3$, shifting pH from 8.0 to 5.0 significantly decreases the $NH_3$ concentration from 5.3 mM to 5.6 $\mu$M, whereas the $NH_4^+$ concentration is virtually unchanged (95−100 mM). Thus, the presence of inhibition at acidic pH without significant pH dependence strongly suggests that $NH_4Cl$-induced $O_2$ inhibition is caused by $NH_4^+$ rather than $NH_3$ in this pH region. This idea was supported by the experiment of changing the $NH_4Cl$ concentration at pH 6.5 (Figure 4). The relative $O_2$ activity as a function of $NH_3$ concentration did not agree with that by pH change (Figure 4B), whereas the plot as a function of $NH_4^+$ concentration was consistent between the pH and $NH_4Cl$ concentration changes (Figure 4C). The $K_i$ value for the inhibition by $NH_4^+$ at pH 6.5 was estimated to be ~160 mM from the plot in Figure 4C, indicative of relatively weak binding of $NH_4^+$ to PSII.

The effect of the $NH_4Cl$ treatment on the $S_2/S_1$ FTIR difference spectrum detected at 283 K showed a good correlation with the $NH_4Cl$ concentration dependence of $O_2$ evolution inhibition (Figure 7). The spectra at both pH 6.5 and pH 5.5 exhibited clear changes in the asymmetric and symmetric $COO^-$ stretching region (Figures 5 and 6). These changes indicate that $NH_4^+$ probably interacts with carboxylate groups, which may serve as ligands to the Mn cluster or proton mediators located in a hydrogen bond network. In the former case, interactions to carboxylate ligands will induce structural perturbations of the Mn cluster that inhibit the proper OEC reactions, while in the latter case, proton release or water insertion processes will be blocked by $NH_4^+$ binding. The appearance of the effects on the $S_2/S_1$ FTIR spectrum indicates that $NH_4^+$ is already bound in the $S_1$ and/or $S_2$ states. Because the $S_1 \rightarrow S_2$ transition is not inhibited as shown in the FTIR difference measurement, actual inhibition should take place in the later S-state transitions such as the $S_2 \rightarrow S_3$ or $S_3 \rightarrow S_0$ transition. Our preliminary FTIR data by applying four successive flashes suggested that the $S_3 \rightarrow S_0$ transition is mainly inhibited in the presence of $NH_4Cl$.

At alkaline pH (pH ~7.5), ammonia inhibition has been extensively studied, and the involvement of neutral $NH_3$ has been established. Three binding sites of $NH_3$ have been proposed.[13,14,19,20] The first site is probably the $Cl^-$ binding site and is related to the $g = 4$ EPR signal, while the second site is thought to be a direct $NH_3$ ligand replacing a substrate water molecule. The direct interaction of $NH_3$ with the Mn cluster has been proposed by the observations of altered multiline EPR signal[15,16] and the ESEEM measurement.[17] The assignment of the altered multiline to neutral $NH_3$ has also been supported by the previous observation[21] that ~10 times higher concentration of $(NH_4)_2SO_4$ was required to detect the altered multiline signal at pH 6.3. We also confirmed that the multiline EPR signal was only slightly modified by 100 mM $NH_4Cl$ treatment at pH 6.5 (Figure 9). However, it has been pointed out that there is no direct correlation between the altered multiline signal and inhibition of $O_2$ evolution,[19,21] and the model has been proposed that the another ammonia molecule slowly bound in the $S_3$ state actually blocks the S-state turnover.[19,20] Because $NH_4^+$ concentration does not much change in the pH 5.0−8.0 range (100−95 mM in the presence of 100 mM $NH_4Cl$), it may be possible that $NH_4^+$ is also involved in the inhibition at the alkaline pH. It could be possible that different factors of inhibition that are dependent on pH result in the absence of specific pH dependence in the inhibition ratio at alkaline pH. Further studies are required to fully understand the mechanism of $NH_4Cl$-induced inhibition in the alkaline region where two possible inhibitors, $NH_3$ and $NH_4^+$, coexist.

MacLachlan et al.[41] previously proposed that $NH_4^+$ inhibits $O_2$ evolution by replacing $Ca^{2+}$ from the observation that the inhibition was decreased by $Ca^{2+}$ addition. However, replacement of $Ca^{2+}$ may not take place in our experiments in which a sufficient amount of $Ca^{2+}$ (20 mM) is always present in buffers. In addition, the FTIR spectral changes by $NH_4^+$ addition observed in the present study are totally different from those by $Ca^{2+}$ depletion, which typically showed the disappearance of the peaks at 1403 and 1364 $cm^{-1}$ in the symmetric $COO^-$ region.[33,42] Thus, the $NH_4^+$ inhibition that we propose here may be unrelated to the previous observation by MacLachlan et al.[41]

The FTIR changes by $NH_4Cl$ treatment detected at 283 K are significantly different from those previously detected at 250 K by Chu and co-workers,[27,28] who showed a clear shift of the positive $COO^-$ peak at 1365 $cm^{-1}$ to 1379 $cm^{-1}$ by addition of 100 mM $NH_4Cl$ to intact PSII membranes at pH 7.5. We observed very similar spectral changes at 250 K using PsbP, PsbQ-depleted PSII membranes treated with 100 mM $NH_4Cl$ at pH 6.5 (Figure 8) and even at pH 5.5 (data not shown). Chu and co-workers[43] also reported that the large shift of the 1365 $cm^{-1}$ band was absent at 277 K, which is consistent with our observation that a large upshift of the ~1365 $cm^{-1}$ band was not observed at 283 K (Figure 5A). The band change at 250 K is saturated already at 100 mM $NH_4Cl$,[27] which is totally different from the concentration dependence of the

$NH_4Cl$ effect on $O_2$ evolution and the FTIR spectrum at 283 K (Figure 7). Thus, it is concluded that the FTIR changes observed at 283 and 250 K have different origins. Chu et al.[27,28] proposed that the FTIR change at 250 K and the altered multiline EPR signal arise from the same $NH_3$ bound to the Mn cluster. However, our observations of the similar FTIR change at 250 K at acid pH (Figure 8) without significant alteration of the multiline EPR signal (Figure 9) suggest the possibility that the FTIR signal at 250 K arises from $NH_4^+$ more likely than $NH_3$. If this is the case, it is possible that $NH_4^+$ bound to the OEC at physiological temperatures is stabilized at a different binding site at 250 K. For a final conclusion about the origin of the FTIR change at 250 K, further experiments to examine the $NH_4Cl$ concentration dependence at different pHs may be necessary.

In conclusion, we have found that $NH_4^+$ functions as an effective inhibitor of $O_2$ evolution in the acidic region around pH 6.5. The interaction of $NH_4^+$ with carboxylate groups at the binding site was detected using FTIR difference spectroscopy. This interaction with carboxylate groups, which may be direct ligands to the Mn cluster or the proton transfer mediators, may cause the inhibition of the OEC reactions. Although it is possible that $NH_4^+$ has a similar inhibitory effect at alkaline pH, the relationship of the $NH_4^+$ inhibition with the well-studied inhibition by $NH_3$ is not clear at present. Further studies are necessary to clarify the detailed mechanism of $NH_4^+$ inhibition including the specific binding site of $NH_4^+$, the S-state transition blocked by $NH_4^+$, and the involvement of $NH_4^+$ in the inhibition at alkaline pH.

## AUTHOR INFORMATION

### Corresponding Author

*Phone: +81-52-789-2881. Fax: +81-52-789-2883. E-mail: tnoguchi@bio.phys.nagoya-u.ac.jp.

### Funding Sources

This study was supported by Grants-in-Aid for Scientific Research from the Ministry of Education, Culture, Sports, Science, and Technology (21108506 and 21370063 to T.N. and 21370069 and 22654051 to H.M.) and Grant-in-Aid for JSPS fellows (224953 to H.S. and 21008983 to T.K.).

## ACKNOWLEDGMENT

The authors thank Miss Chihiro Uno for technical assistance in SDS−PAGE analysis. We also thank Drs. Alain Boussac, Gary W. Brudvig, and Hsiu-An Chu for stimulating discussions and Dr. Gernot Renger for careful reading of the manuscript.

## ABBREVIATIONS

EPR, electron paramagnetic resonance; ESEEM, electron spin echo envelope modulation; EXAFS, extended X-ray absorption fine structure; FTIR, Fourier transform infrared; Hepes, 4-(2-hydroxyethyl)-1-piperazineethanesulfonic acid; Mes, 2-(*N*-morpholino)ethanesulfonic acid; OEC, oxygen evolving center; P*p*BQ, phenyl-*p*-benzoquinone; PSII, photosystem II.

## ADDITIONAL NOTE

[a]An X-ray crystallographic structure of the PSII complexes from *Thermosynechococcus vulcanus* at 1.9 Å resolution was recently reported by Shen and co-workers at the 15th International Congress of Photosynthesis in Beijing (PS6.5).

## REFERENCES

(1) Debus, R. J. (1992) The manganese and calcium ions of photosynthetic oxygen evolution. *Biochim. Biophys. Acta 1102*, 269–352.

(2) Hillier, W., and Messinger, J. (2005) Mechanism of photosynthetic oxygen production, in *Photosystem II: The Light-Driven Water: Plastoquinone Oxidoreductase* (Wydrzynski, T., and Satoh, K., Eds.) pp 567−608, Springer, Dordrecht, The Netherlands.

(3) McEvoy, J. P., and Brudvig, G. W. (2006) Water-splitting chemistry of photosystem II. *Chem. Rev. 106*, 4455–4483.

(4) Renger, G. (2007) Oxidative photosynthetic water splitting: energetics, kinetics and mechanism. *Photosynth. Res. 92*, 407–425.

(5) Ferreira, K. N., Iverson, T. M., Maghlaoui, K., Barber, J., and Iwata, S. (2004) Architecture of the photosynthetic oxygen-evolving center. *Science 303*, 1831–1838.

(6) Guskov, A., Kern, J., Gabdulkhakov, A., Broser, M., Zouni, A., and Saenger, W. (2009) Cyanobacterial photosystem II at 2.9-Å resolution and the role of quinones, lipids, channels and chloride. *Nat. Struct. Mol. Biol. 16*, 334–342.

(7) Kawakami, K., Umena, Y., Kamiya, N., and Shen, J.-R. (2009) Location of chloride and its possible functions in oxygen-evolving photosystem II revealed by X-ray crystallography. *Proc. Natl. Acad. Sci. U.S.A. 106*, 8567–8572.

(8) Yano, J., Kern, J., Sauer, K., Latimer, M. J., Pushkar, Y., Biesiadka, J., Loll, B., Saenger, W., Messinger, J., Zouni, A., and Yachandra, V. K. (2006) Where water is oxidized to dioxygen: Structure of the photosynthetic $Mn_4Ca$ cluster. *Science 314*, 821–825.

(9) Hind, G., and Whittingham, C. P. (1963) Reduction of ferricyanide by chloroplasts in presence of nitrogenous bases. *Biochim. Biophys. Acta 75*, 194–202.

(10) Izawa, S., Heath, R. L., and Hind, G. (1969) The role of chloride ion in photosynthesis III. The effect of artificial electron donors upon electron transport. *Biochim. Biophys. Acta 180*, 388–398.

(11) Velthuys, B. R. (1975) Binding of inhibitor $NH_3$ to oxygen-evolving apparatus of spinach chloroplasts. *Biochim. Biophys. Acta 396*, 392–401.

(12) Ono, T., and Inoue, Y. (1988) Abnormal S-state turnovers in $NH_3$-binding Mn centers of photosynthetic $O_2$ evolving system. *Arch. Biochem. Biophys. 264*, 82–92.

(13) Sandusky, P. O., and Yocum, C. F. (1984) The chloride requirement for photosynthetic oxygen evolution—Analysis of the effects of chloride and other anions on amine inhibition of the oxygen-evolving complex. *Biochim. Biophys. Acta 766*, 603–611.

(14) Sandusky, P. O., and Yocum, C. F. (1986) The chloride requirement for photosynthetic oxygen evolution: factors affecting nucleophilic displacement of chloride from the oxygen-evolving complex. *Biochim. Biophys. Acta 849*, 85–93.

(15) Beck, W. F., de Paula, J. C., and Brudvig, G. W. (1986) Ammonia binds to the manganese site of the $O_2$-evolving complex of photosystem II in the $S_2$ state. *J. Am. Chem. Soc. 108*, 4018–4022.

(16) Beck, W. F., and Brudvig, G. W. (1986) Binding of amines to the $O_2$-evolving center of photosystem II. *Biochemistry 25*, 6479–6486.

(17) Britt, R. D., Zimmermann, J.-L., Sauer, K., and Klein, M. P. (1989) Ammonia binds to the catalytic Mn of the oxygen-evolving complex of photosystem II: Evidence by electron-spin echo envelope modulation spectroscopy. *J. Am. Chem. Soc. 111*, 3522–3532.

(18) Dau, H., Andrews, J. C., Roelofs, T. A., Latimer, M. J., Liang, W. C., Yachandra, V. K., Sauer, K., and Klein, M. P. (1995) Structural consequences of ammonia binding to the manganese center of the photosynthetic oxygen-evolving complex: an X-ray absorption spectroscopy study of isotropic and oriented photosystem II particles. *Biochemistry 34*, 5274–5287.

(19) Boussac, A., Rutherford, A. W., and Styring, S. (1990) Interaction of ammonia with the water splitting enzyme of photosystem II. *Biochemistry 29*, 24–32.

(20) Boussac, A., Sugiura, M., Inoue, Y., and Rutherford, A. W. (2000) EPR study of the oxygen evolving complex in His-tagged photosystem II from the cyanobacterium *Synechococcus elongates*. *Biochemistry 39*, 13788–13799.

(21) Andréasson, L.-E., Hansson, Ö., and von Schenck, K. (1988) The interaction of ammonia with the photosynthetic oxygen-evolving system. *Biochim. Biophys. Acta 936*, 351–360.

(22) Chu, H.-A., Hillier, W., Law, N. A., and Babcock, G. T. (2001) Vibrational spectroscopy of the oxygen-evolving complex and of manganese model compounds. *Biochim. Biophys. Acta 1503*, 69–82.

(23) Noguchi, T., and Berthomieu, C. (2005) Molecular analysis by vibrational spectroscopy, in *Photosystem II: The Light-Driven Water: Plastoquinone Oxidoreductase* (Wydrzynski, T., and Satoh, K., Eds.) pp 367−387, Springer, Dordrecht, The Netherlands.

(24) Noguchi, T. (2007) Light-induced FTIR difference spectroscopy as a powerful tool toward understanding the molecular mechanism of photosynthetic oxygen evolution. *Photosynth. Res. 91*, 59–69.

(25) Noguchi, T. (2008) Fourier transform infrared analysis of the photosynthetic oxygen-evolving center. *Coord. Chem. Rev. 252*, 336–346.

(26) Debus, R. J. (2008) Protein ligation of the photosynthetic oxygen-evolving center. *Coord. Chem. Rev. 252*, 244–258.

(27) Chu, H.-A., Feng, Y.-W., Wang, C.-M., Chiang, K.-A., and Ke, S.-C. (2004) Ammonia-induced structural changes of the oxygen-evolving complex in photosystem II as revealed by light-induced FTIR difference spectroscopy. *Biochemistry 43*, 10877–10885.

(28) Fang, C.-H., Chiang, K.-A., Hung, C.-H., Chang, K., Ke, S.-C., and Chu, H.-A. (2005) Effects of ethylene glycol and methanol on ammonia-induced structural changes of the oxygen-evolving complex in photosystem II. *Biochemistry 44*, 9758–9765.

(29) Berthold, D. A., Babcock, G. T., and Yocum, C. F. (1981) A highly resolved, oxygen-evolving photosystem II preparation from spinach thylakoid membranes. EPR and electron-transport properties. *FEBS Lett. 134*, 231–234.

(30) Ono, T., and Inoue, Y. (1986) Effects of removal and reconstitution of the extrinsic 33, 24 and 16 kDa proteins on flash oxygen yield in photosystem II particles. *Biochim. Biophys. Acta 850*, 380–389.

(31) Åkerlund, H.-E., Jansson, C., and Andersson, B. (1982) Reconstitution of photosynthetic water splitting in inside-out thylakoid vesicles and identification of a participating polypeptide. *Biochim. Biophys. Acta 681*, 1–10.

(32) Suzuki, H., Taguchi, Y., Sugiura, M., Boussac, A., and Noguchi, T. (2006) Structural perturbation of the carboxylate ligands to the manganese cluster upon $Ca^{2+}/Sr^{2+}$ exchange in the S-state cycle of photosynthetic oxygen evolution as studied by flash-induced FTIR difference spectroscopy. *Biochemistry 45*, 13454–13464.

(33) Noguchi, T., Ono, T., and Inoue, Y. (1995) Direct detection of a carboxylate bridge between Mn and $Ca^{2+}$ in the photosynthetic oxygen-evolving center by means of Fourier transform infrared spectroscopy. *Biochim. Biophys. Acta 1228*, 189–200.

(34) Vass, I., and Styring, S. (1991) pH-Dependent charge equilibria between tyrosine-D and the S states in photosystem II. Estimation of relative midpoint redox potentials. *Biochemistry 30*, 830–839.

(35) Kuntzleman, T. S., and Haddy, A. (2009) Fluoride inhibition of photosystem II and the effect of removal of the PsbQ subunit. *Photosynth. Res. 102*, 7–19.

(36) Ifuku, K., and Sato, F. (2001) Importance of the N-terminal sequence of the extrinsic 23 kDa polypeptide in photosystem II in ion retention in oxygen evolution. *Biochim. Biophys. Acta 1546*, 196–204.

(37) Noguchi, T., and Sugiura, M. (2003) Analysis of flash-induced FTIR difference spectra of the S-state cycle in the photosynthetic water-oxidizing complex by uniform $^{15}N$ and $^{13}C$ isotope labeling. *Biochemistry 42*, 6035–6042.

(38) Kimura, Y., Mizusawa, N., Ishii, A., Yamanari, T., and Ono, T. (2003) Changes of low-frequency vibrational modes induced by universal $^{15}N$- and $^{13}C$-isotope labeling in $S_2/S_1$ FTIR difference spectrum of oxygen-evolving complex. *Biochemistry 42*, 13170–13177.

(39) Tomita, M., Ifuku, K., Sato, F., and Noguchi, T. (2009) FTIR evidence that the PsbP extrinsic protein induces protein conformational changes around the oxygen-evolving Mn cluster in photosystem II. *Biochemistry 48*, 6318–6325.

(40) Noguchi, T., and Inoue, Y. (1995) Identification of FTIR signals from the non-heme iron in photosystem II. *J. Biochem. 118*, 9–12.

(41) MacLachlan, D. J., Nugent, J. H. A., Warden, J. T., and Evans, M. C. W. (1994) Investigation of the ammonium chloride and ammonium acetate inhibition of oxygen evolution by photosystem II. *Biochim. Biophys. Acta 1188*, 325–334.

(42) Taguchi, Y., and Noguchi, T. (2007) Drastic changes in the ligand structure of the oxygen-evolving Mn cluster upon $Ca^{2+}$ depletion as revealed by FTIR difference spectroscopy. *Biochim. Biophys. Acta 1767*, 535–540.

(43) Huang, H.-H., Wang, T.-H., and Chu, H.-A. (2008) Ammonia-induced structural changes of oxygen-evolving complex in photosystem II diminished at 277 K as revealed by light-induced FTIR difference spectroscopy, in *Photosynthesis. Energy from the Sun: 14th International Congress on Photosynthesis* (Allen, J. F., Gantt, E., Golbeck, J. H., and Osmond, B., Eds.) pp 389−391, Springer, Dordrecht, The Netherlands.